

Quasar emission lines as virial luminosity estimators

P. Marziani¹, E. Bon², N. Bon², M.L. Martinez-Aldama³,
G.M. Stirpe⁴, M. D’Onofrio⁵, A. del Olmo⁶, C.A. Negrete⁷
and D. Dultzin⁷

¹ National Institute for Astrophysics (INAF), Padua Astronomical Observatory, Padua, (E-mail: paola.marziani@inaf.it)
Italy

² Astronomical Observatory, Belgrade, Serbia

³ Center for Theoretical Physics, Polish Academic of Sciences, Warsaw, Poland

⁴ INAF - Osservatorio Astrofisica e Science dello Spazio, Bologna, Italy

⁵ Dipartimento di Fisica ed Astronomia “Galileo Galilei,” Università di Padova, Padova, Italia

⁶ Instituto de Astrofísica de Andalucía (CSIC), Granada, Spain

⁷ Instituto de Astronomía, UNAM, Mexico, D.F., Mexico

Received: July 30, 2019 ; Accepted: August 22, 2019

Abstract. Quasars accreting matter at very high rates (known as extreme Population A [xA]) may provide a new class of distance indicators covering cosmic epochs from present day up to less than 1 Gyr from the Big Bang. We report on the developments of a method that is based on “virial luminosity” estimates from measurements of emission line widths of xA quasars. The approach is conceptually equivalent to the virial estimates based on early and late type galaxies. The main issues related to the cosmological application of luminosity estimates from xA quasar line widths are the identification of proper emission lines whose broadening is predominantly virial over a wide range of luminosity, and the assessment of the effect of the emitting region orientation with respect to the line of sight. We report on recent developments concerning the use of the AlIII λ 1860 intermediate ionisation line and of the Hydrogen Balmer line H β as “virial broadening estimators.”

1. Introduction: a main sequence for quasars

The Main Sequence (MS) is a powerful tool to organize type-1 quasar diversity (see e.g., Marziani et al., 2018, for a recent review). The MS concept originated from the first eigenvector (E1) of a Principal Component Analysis carried out on a sample of ≈ 80 Palomar-Green quasars (Boroson & Green, 1992). The E1 MS was first associated with anti-correlations between strength of FeII λ 4570 and width of H β as well as strength of FeII λ 4570 and [OIII] prominence. Over

the years, several parameters related to the accretion process and the accompanying outflows were found to be also associated with the fundamental relation between prominence of singly-ionized iron emission and broad Balmer line width (Sulentic et al., 2000, 2007). For an exhaustive list see Sulentic et al. (2011); Fraix-Burnet et al. (2017). Since 1992, the E1 MS has been found in increasingly larger samples, and the MS potential was fully recognized following an SDSS-based analysis of a large sample of several tens of thousands of quasars (Shen & Ho, 2014).

The optical plane of the MS is defined by the FWHM of the $H\beta$ broad component vs the parameter R_{FeII} that is defined as $R_{\text{FeII}} = I(\text{FeII}\lambda 4570)/I(H\beta)$, the ratio between the integrated flux of the FeII $\lambda 4570$ blend of multiplets, and that of the $H\beta$ broad component (Sulentic et al., 2000). The data are distributed as an elbow-shaped figure (Fig. 1) if a restriction to low- z and relatively low luminosity is applied; if higher luminosity sources are included the MS takes a wedge-like form (as in case of Shen & Ho 2014).

It is not surprising that a measure of FeII emission can lead a fundamental correlation, as singly-ionized emission is extended from the UV to the NIR, and can dominate the thermal balance of the broad line region (BLR, Marinello et al., 2016). FeII emission is self-similar but its intensity with respect to Hydrogen Balmer line $H\beta$ changes. The width of $H\beta$ is mainly associated with the broadening due to the emitting gas dynamics via Doppler effect. A correlation between the two parameters points towards a coupling between physical and dynamical conditions within the line emitting region, as further discussed in § 2.

Quasar spectra show a wide range of line profiles, line shifts, line intensities and differences in dynamical conditions and ionization levels of the BLR, systematically changing along the sequence. It is expedient to identify spectral types along the MS (Fig. 1) and to distinguish between Population A ($\text{FWHM}(H\beta) \leq 4000 \text{ km s}^{-1}$) and Population B ($\text{FWHM}(H\beta) > 4000 \text{ km s}^{-1}$). Pop. A sources include prototypical Narrow Line Seyfert 1 IZw1 as well as sources with relatively little FeII, such as Mark 335. The appearance of the spectrum suggests a relatively low degree of ionization, with significant FeII, weak [OIII] $\lambda\lambda 4959, 5007$ and weak high-ionization lines in general. Pop. B objects show not only broader lines but also higher ionization, weak FeII and strong [OIII]. A prototypical source is NGC 5548 (Sulentic et al., 2000). Regarding internal line shifts in the spectra of individual quasars, it is helpful to distinguish between low- and high-ionization lines (HILs and LILs). Internal line shifts between HILs and LILs are mainly associated with HIL blueshifted emission.

The MS is probably due to a combination of effects dependent on Eddington ratio, viewing angle, and metal content (Panda et al. 2019 and references therein). The connection between observational and accretion parameters is not well-mapped as yet, but the quasar MS could be aptly considered as the analogous of the MS in the stellar H-R diagram (Sulentic et al., 2001, 2008).

Even if our understanding is not complete, it is possible to exploit some well-defined properties in particular sectors “spectral types” along the MS. A second key element that makes it possible to consider quasars even as “Eddington standard candles” (i.e., sources with a small scatter around a fixed value of the Eddington ratio in place of a luminosity measure) has been the ability to recognize that the part of the BLR emitting the LIL is eminently virialized. In the following we will summarize in which way quasar emission lines can be considered as virial broadening estimators (VBE, §2) and identify a particular class of quasars (§3) for which the assumption of an almost constant Eddington ratio is likely to be verified. We stress the analogy with stellar systems (§4.1) and consider redshift-independent estimates of luminosity made possible by the scaling between virial broadening and luminosity itself (§5).

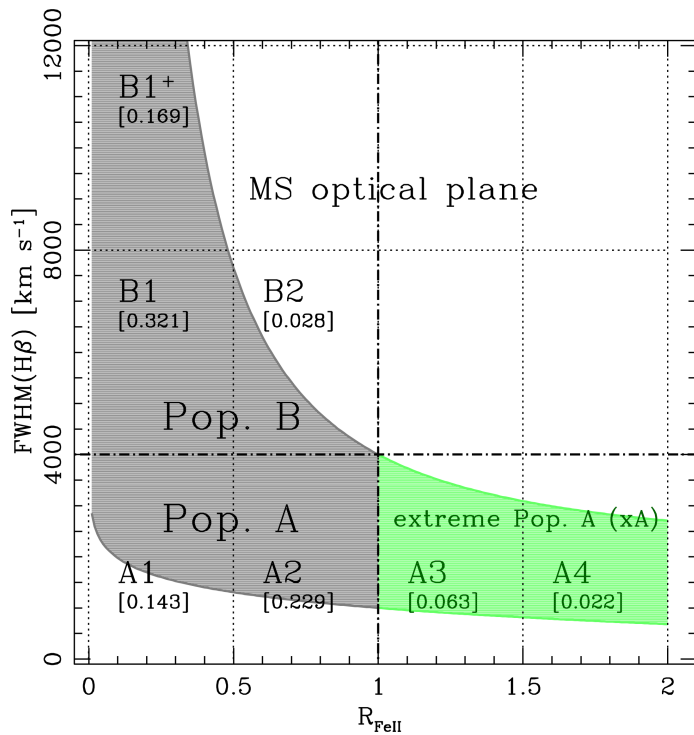


Figure 1. A sketch outlining the occupation of optical plane of the quasar MS. The plane has been subdivided in spectral types, and the region of extreme Population A has been shaded green. The numbers in square brackets are the relative prevalence in the ST along the sequence, from the sample of Marziani et al. (2013a).

2. A virialized and a wind system

The origin of the broadening of quasar emission lines has been a contentious issue for decades after quasar discovery and it is as yet not fully understood. Reverberation-mapping campaign have provided direct evidence of a large mass concentration in a very small volume of space, with broadening for lines emitted by different ionic species becoming larger and their distance decreasing with increasing ionisation potential (Peterson & Wandel, 1999). At the same time, internal line shifts (measured soon after the quasar discovery, Burbidge & Burbidge 1967) complicated the interpretation of the spectra of individual quasars. A turning point was the ability offered by the FOS on board HST to observe the HIL CIV 1549 and to compare it to a strong LIL such as H β (Corbin & Boroson, 1996; Marziani et al., 1996). It was found that the CIV line showed prominent blueshift while the H β remained almost unshifted with respect to the rest frame of the quasars. If we assume that a line whose profile appears symmetric and unshifted with respect to rest frame can be considered as a marker of a virialized emitting region, this result provided support to the idea that the BLR were composed of two sub-regions, one emitting predominantly HIL in an outflow scenario and one associated with a flattened distribution of gas coplanar with the accretion disk (possibly the accretion disk itself, Collin-Souffrin et al. 1988; Elvis 2000; see Fig. 2). Later, it was found that a virialized system emitting mainly LILs coexists with outflowing gas in Pop. A sources, even at the highest luminosity (Sulentic et al., 2017; Vietri, 2017; Coatman et al., 2017).

3. Extreme Population A

Selection and physical conditions of Extreme Population A is made possible by the MS that allows for the definition of spectral types, in addition to the two Populations defined earlier. Spectral types within Pop. A are due to a gradient of R_{FeII} (Boroson & Green, 1992; Sulentic et al., 2000; Shen & Ho, 2014; Du et al., 2016; Panda et al., 2019).

Extreme Pop. A quasars (xA) are selected applying simple criteria from diagnostic emission line intensity ratios:

1. $R_{\text{FeII}} \text{ FeII}\lambda 4570 \text{ blend}/\text{H}\beta \gtrsim 1.0$;
2. UV AlIII $\lambda 1860/\text{SiIII}[\lambda 1892] \gtrsim 0.5$ and $\text{SiIII}[\lambda 1892]/\text{CIII}[\lambda 1909] \gtrsim 1$

UV and optical selection criteria are equivalent, and lead to the identification as xA of $\sim 10\%$ of all quasars in low- z , optically selected samples. xA spectra show distinctively strong FeII emission and Lorentzian Balmer line profiles, and $\text{FWHM}(\text{H}\beta) \approx \text{FWHM}(\text{AlIII} 1860)$ whenever it has been possible to cover both lines for the same object (Negrete et al. 2013; Marziani & Sulentic 2014). This means that the AlIII 1860 FWHM is a virial broadening estimator equivalent to H β (del Olmo et al. 2019, in preparation). The measurements of the 1900 blend

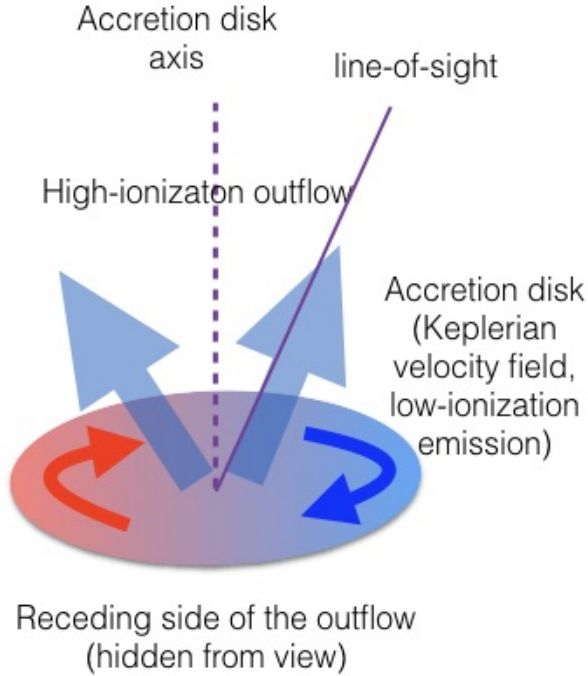


Figure 2. A sketch illustrating the principle of a virialized sub-region co-existing with an outflowing component. The sketch is highly simplified and accounts for the systematic blueshifts of HILs, large when the HI Balmer lines are narrower, but does not take into account the systematic changes in accretion modes expected along the sequence.

and specifically of the AlIII line allows for the consideration of xA quasars at high z ($\gtrsim 1.2$).

The UV spectrum of xA quasars at $z \sim 2$ shows symmetric low-ionization and blueshifted high-ionization lines even at the highest luminosity (Martínez-Aldama et al. 2018, and reference therein). The CIV and the 1900 blend lines have low equivalent width: about one-half of xAs are weak lined quasars following the definition of Diamond-Stanic et al. (2009).

Observed diagnostic ratios (CIV/AlIII, CIV/HeII, AlIII/SiIII) imply extreme values for density (high, $n \gtrsim 10^{12-13} \text{ cm}^{-3}$), ionization (low, $U \sim 10^{-3}$) and extreme values of metallicity ($Z \gtrsim 20Z_{\odot}$, Martínez-Aldama et al. 2018, Sniegowska et al. 2019 in preparation). These values are inferred by considering curves of constant intensity ratios in the plane ionization parameter versus density from arrays of CLOUDY simulations (Negrete et al., 2012). A crossing

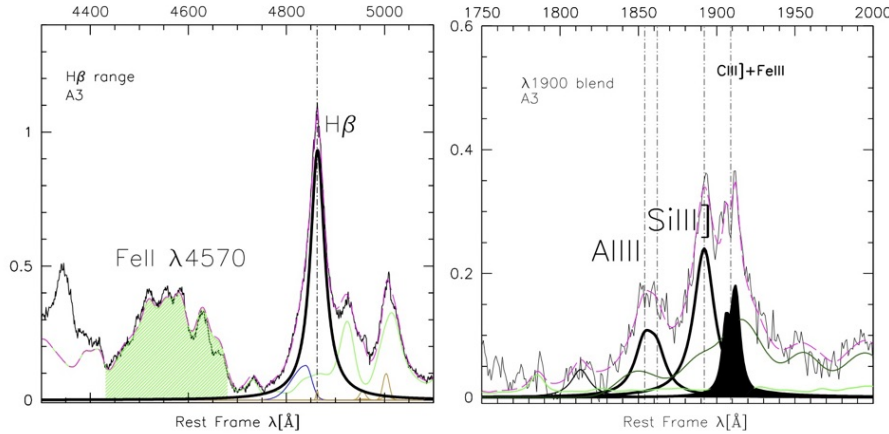


Figure 3. Examples of the H β (left, Marziani et al. 2013b) and 1900 Å (right, Bachev et al. 2004) spectral region (after continuum subtraction) in low redshift extreme Eddington candidates, selected from the optical criterion $R_{\text{FeII}} > 1$. The ratio R_{FeII} is obtained by measuring the flux of the FeII blend at 4570 Å (pale green shaded area), and the flux of H β . The thick black lines trace broad lines whose FWHM can be used as virial broadening estimator, AlIIIλ1860, SiIII]λ1892, and H β but not CIII]λ1909 (shaded dark). H β and the UV lines have been found to provide consistent FWHM measures in agreement with H β at low- L . Green lines show FeII templates (pale), and the FeIII template in the UV (dark). The magenta dashed lines show models of the total line emission.

point defined by the isopleth of constant intensity ratios identifies the physical conditions that predict all considered intensity ratios. The very high density inferred from the weakness of CIII]λ1909, and the maximum radiative output per unit mass suggests that the LIL Emitting regions could be a dense compact remnant of a more conventional LIL-BLR.

4. Extreme Population A quasars: virial broadening

There are several lines of evidence suggesting that the R_{FeII} is correlated with Eddington ratio. Among them, we mention the fundamental plane of the accretion black holes correlations (Du et al., 2016) which is a restatement of the correlation of Eddington ratio R_{FeII} , adding a second correlate associated with the LIL profile. Extreme Population A ($R_{\text{FeII}} \gtrsim 1$) show extreme L/L_{Edd} along the MS with small dispersion (Marziani & Sulentic, 2014) (MS14). Accretion disk theory predicts low radiative efficiency at high accretion rate; L/L_{Edd} saturates toward a limiting values; (Minehige et al., 2000; Abramowicz et al., 1988; Sadowski, 2011). This seems to be what is occurring to xA sources.

A virial luminosity estimate for large samples of xA quasars is possible if:

1. xA quasars radiate close to Eddington limit $L/L_{\text{Edd}} \propto L/M_{\text{BH}} \sim 1$. The exact value of the the Eddington ratio is not relevant, provided that L/L_{Edd} scatters little around a well-defined value. At this point we are able to recognize only xA quasars at one extreme of the MS, but the same approach could be applied to other sources along the MS, were their Eddington ratio known with high precision.
2. Virial motions are the broadening source of the low-ionization BLR.
3. xA quasars have similar BLR physical parameters, an assumption that is justified by the spectral similarity over a large range in luminosity. This implies that BLR radius rigorously scales with the square root of the luminosity.

If we know a virial broadening estimator δv (in practice, the FWHM of a low- ionization line), we can derive a z -independent, “virial” luminosity, $L_{\text{vir}} \propto (n_{\text{H}} U)^{-1} (\delta v)^4$. The virial luminosity can be written as $L = L_0 \text{ FWHM}^4$, where the constant depends on the fraction of ionizing luminosity, the average frequency of ionizing photons, and the photon flux. These are all intrinsic properties of quasars.

4.1. $L \propto (\delta v)^a$: not only for quasars

The $L \propto \text{FWHM}^4$ is a law analogous to the Tully-Fisher and the early formulation of the Faber Jackson laws for early- type galaxies (Faber & Jackson, 1976; Tully & Fisher, 1977). Galaxies and even clusters of galaxies are virialized systems that globally follows a law $\propto \sigma^4$ (Fig. 4). The main difference with quasars is that the velocity dispersion of stellar system is by far not as strongly dependent on the viewing angle as the FWHM of quasar LILs.

5. Interpretation of the virial luminosity estimates for quasars

5.1. Virial luminosity and redshift-based luminosity

The sketch of Fig. 2 suggests that the viewing angle of the plane of the accretion disk should substantially affect the projection of the virial velocity field along the line-of-sight. In other words, the FWHM is strongly dependent on the viewing angle θ defined as the angle between the line of sight and the axis of the accretion disk plane.

The virial luminosity is applicable to xA quasars over a wide range of luminosity and redshift. If we compare the virial luminosity to the conventional estimate of luminosity from redshift, H_0 and the Ω_s we find that there is an overall consistency with redshift-based concordance luminosity. At the same time we

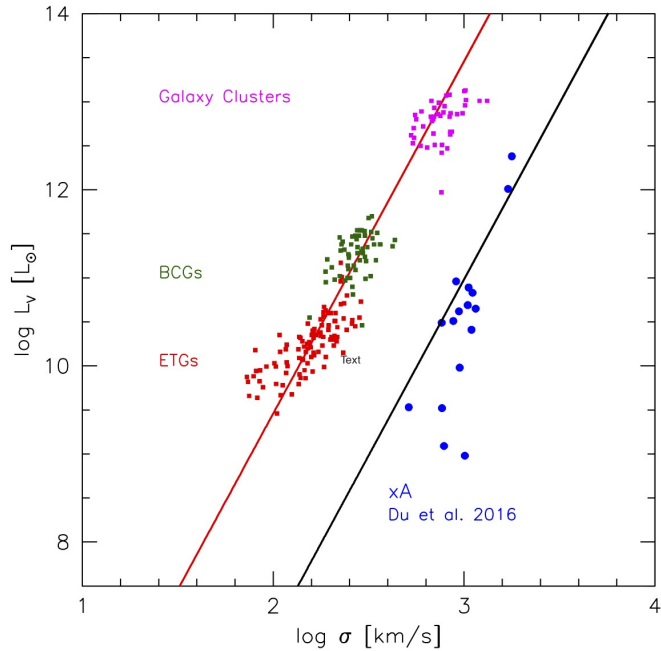


Figure 4. Relation between virial broadening and luminosity, for several classes of virialized stellar systems and quasars. Data points refers to early-type galaxies (ETGs, red squares), brightest cluster galaxies (BCGs, dark-green squares), clusters of galaxies (magenta squares) from the wide-field nearby galaxy-cluster survey and are as used in D’Onofrio et al. (2019), and xA quasars from the sample of Du et al. (2016). The filled lines trace two relations with $L \propto \sigma^4$.

measure a significant scatter $\sigma \sim 0.5$ dex (Fig. 5; 0.3 dex can be reached by improving the statistics of larger samples, as done in Marziani et al. 2017, but a substantial statistical scatter is expected to remain even in large samples of excellent data).

An analysis aimed at the cosmological exploitation of the virial luminosity is ongoing. Work to improve the accuracy of black hole mass and Eddington ratio using θ is also in progress. At this point, however, it is perhaps more interesting to try to understand the origin of the scatter between virial luminosity and conventional luminosity $L(z, H_0, \Omega_M, \Omega_\Lambda)$, where the cosmological parameter have been assumed to have values consistent with the concordance ones.

The difference between the virial L and $L(z, H_0, \Omega_M, \Omega_\Lambda)$ as a function of redshift for the sample of Negrete et al. (2018) is shown in the left panel of Fig. 5. The scatter is due in part to measurement errors. The FWHM enters to the fourth power in the L expression; a 10% error, achievable with high S/N

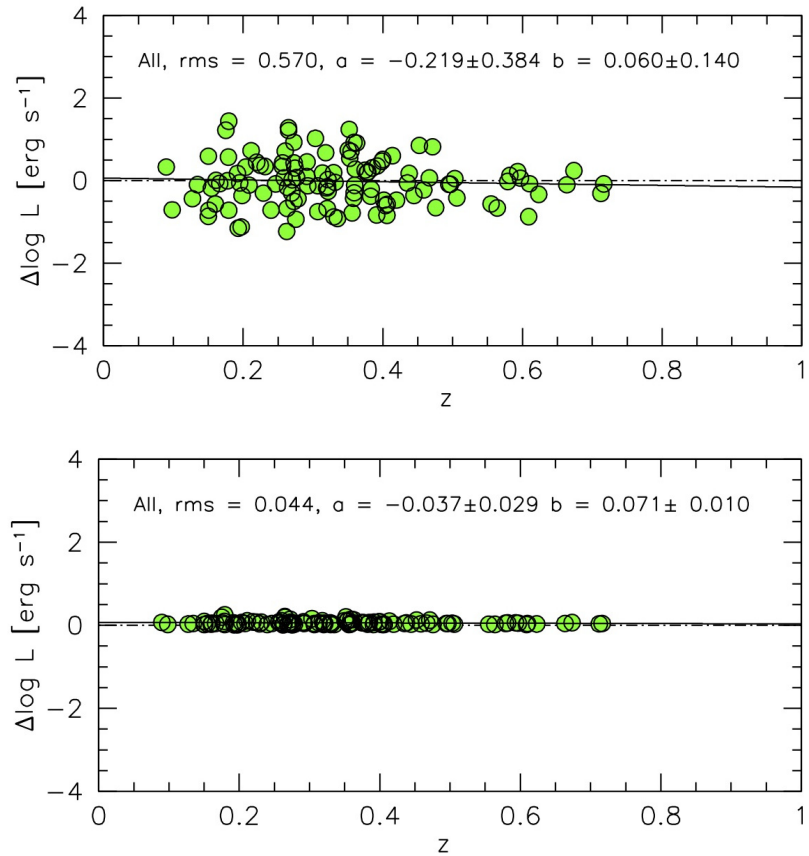


Figure 5. Quasar luminosity estimates: residuals as a function of redshift z of virial luminosity estimated from the $H\beta$ FWHM minus luminosity $L(z, H_0, \Omega_M, \Omega_\Lambda)$ from redshift before orientation correction (above), and after (below). Data are from the low- z quasar sample of Negrete et al. (2018).

data would imply a ≈ 0.17 dex error on luminosity (see Marziani & Sulentic 2014 for a preliminary error budget). More than measurement errors, it is likely that orientation accounts for most of the scatter, especially if lines are emitted in a flattened system. There is growing evidence that this is the case (Mejía-Restrepo et al., 2018; Afanasiev et al., 2019; Marziani et al., 2019) although the expression of the form factor connecting virial velocity and projected broadening is still debated. Assuming a structure factor f relating virial broadening δv_K and line FWHM ($\delta v_K^2 = f \text{FWHM}^2$) in the form $f = 1/4(\kappa^2 + \sin^2 \theta)$, where κ can be interpreted as the ratio between an isotropic velocity component and the

virial velocity, we found that all objects in the sample of Negrete et al. (2018) can be accounted for by the effect of the viewing angle within $0 \lesssim \theta \lesssim 50$ degrees (in the right panel of Fig. 5 residuals are zeroed if $f^{1/2}\text{FWHM}$ is used as a VBE). Orientation might be really the main source of scatter between virial and conventional luminosity estimates. More details are given by Negrete et al. (2018), and a more conclusive analysis will be hopefully presented in forthcoming studies.

6. Conclusion

The MS offer contextualization of quasar observational and physical properties. Extreme Population A (xA) quasars at the high R_{FeII} end of the MS appear to radiate at extreme L/L_{Edd} . xA quasars show a relatively high prevalence (10%) and are easily recognizable. Low ionization lines are apparently emitted in a highly-flattened, virialized BLR, and the consistency between virial and redshift-based luminosity estimates supports this basic interpretation also for xA quasars. Several methods to derive redshift-independent L values based on intrinsic properties of quasars have been proposed in the last few years (Wang et al., 2013; La Franca et al., 2014; Risaliti & Lusso, 2015); xA quasars might be suitable as “Eddington standard candles” especially if orientation effects can be accounted for.

Acknowledgements. PM and MDO acknowledge funding from the INAF PRIN-SKA 2017 program 1.05.01.88.04. PM is also grateful for support via a STSM of the COST Action CA16104, Gravitational waves, black holes and fundamental physics that allowed her participation to the SCSLSA12. AdO acknowledges financial support from the Spanish Ministry of Economy and Competitiveness through grant AYA2016-76682-C3-1-P and from the State Agency for Research of the Spanish MCIU through the Center of Excellence Severo Ochoa award for the Instituto de Astrofísica de Andalucía (SEV-2017-0709). E.B. and N.B. acknowledge support from the Ministry of Education, Science and Technological Development of the Republic of Serbia through the projects Astrophysical Spectroscopy of Extragalactic Objects (176001) and Gravitation and structure of the Universe on large scales (176003).

References

- Abramowicz, M. A., Czerny, B., Lasota, J. P., & Szuszkiewicz, E., Slim accretion disks. 1988, *Astrophys. J.*, **332**, 646, DOI: 10.1086/166683
- Afanasiev, V. L., Popović, L. Č., & Shapovalova, A. I., Spectropolarimetry of Seyfert 1 galaxies with equatorial scattering: black hole masses and broad-line region characteristics. 2019, *Mon. Not. R. Astron. Soc.*, **482**, 4985, DOI: 10.1093/mnras/sty2995
- Bachev, R., Marziani, P., Sulentic, J. W., et al., Average Ultraviolet Quasar Spectra in the Context of Eigenvector 1: A Baldwin Effect Governed by the Eddington Ratio? 2004, *ApJ*, **617**, 171, DOI: 10.1086/425210

- Boroson, T. A. & Green, R. F., The emission-line properties of low-redshift quasi-stellar objects. 1992, *ApJS*, **80**, 109, DOI: 10.1086/191661
- Burbidge, G. R. & Burbidge, E. M. 1967, *Quasi-stellar objects* (San Francisco, Freeman)
- Coatman, L., Hewett, P. C., Banerji, M., et al., Correcting C IV-based virial black hole masses. 2017, *Mon. Not. R. Astron. Soc.*, **465**, 2120, DOI: 10.1093/mnras/stw2797
- Collin-Souffrin, S., Dyson, J. E., McDowell, J. C., & Perry, J. J., The environment of active galactic nuclei. I - A two-component broad emission line model. 1988, *MNRAS*, **232**, 539
- Corbin, M. R. & Boroson, T. A., Combined Ultraviolet and Optical Spectra of 48 Low-Redshift QSOs and the Relation of the Continuum and Emission-Line Properties. 1996, *Astrophys. J., Suppl.*, **107**, 69, DOI: 10.1086/192355
- Diamond-Stanic, A. M., Fan, X., Brandt, W. N., et al., High-redshift SDSS Quasars with Weak Emission Lines. 2009, *Astrophys. J.*, **699**, 782, DOI: 10.1088/0004-637X/699/1/782
- D'Onofrio, M., Sciarratta, M., Cariddi, S., Marziani, P., & Chiosi, C., The Parallelism between Galaxy Clusters and Early-type Galaxies. I. The Light and Mass Profiles. 2019, *Astrophys. J.*, **875**, 103, DOI: 10.3847/1538-4357/ab1134
- Du, P., Wang, J.-M., Hu, C., et al., The Fundamental Plane of the Broad-line Region in Active Galactic Nuclei. 2016, *Astrophys. J., Lett.*, **818**, L14, DOI: 10.3847/2041-8205/818/1/L14
- Elvis, M., A Structure for Quasars. 2000, *Astrophys. J.*, **545**, 63, DOI: 10.1086/317778
- Faber, S. M. & Jackson, R. E., Velocity dispersions and mass-to-light ratios for elliptical galaxies. 1976, *Astrophys. J.*, **204**, 668, DOI: 10.1086/154215
- Fraix-Burnet, D., Marziani, P., D'Onofrio, M., & Dultzin, D., The Phylogeny of Quasars and the Ontogeny of Their Central Black Holes. 2017, *Frontiers in Astronomy and Space Sciences*, **4**, 1, DOI: 10.3389/fspas.2017.00001
- La Franca, F., Bianchi, S., Ponti, G., Branchini, E., & Matt, G., A New Cosmological Distance Measure Using Active Galactic Nucleus X-Ray Variability. 2014, *Astrophys. J., Lett.*, **787**, L12, DOI: 10.1088/2041-8205/787/1/L12
- Marinello, M., Rodríguez-Ardila, A., García-Rissmann, A., Sigut, T. A. A., & Pradhan, A. K., The Fe II Emission in Active Galactic Nuclei: Excitation Mechanisms and Location of the Emitting Region. 2016, *Astrophys. J.*, **820**, 116, DOI: 10.3847/0004-637X/820/2/116
- Martínez-Aldama, M. L., Del Olmo, A., Marziani, P., et al., Highly Accreting Quasars at High Redshift. 2018, *Frontiers in Astronomy and Space Sciences*, **4**, 65, DOI: 10.3389/fspas.2017.00065
- Marziani, P., del Olmo, A., Martínez-Carballo, M. A., et al., Black hole mass estimates in quasars. A comparative analysis of high- and low-ionization lines. 2019, *Astron. Astrophys.*, **627**, A88, DOI: 10.1051/0004-6361/201935265
- Marziani, P., Dultzin, D., Sulentic, J. W., et al., A main sequence for quasars. 2018, *Frontiers in Astronomy and Space Sciences*, **5**, 6

- Marziani, P., Negrete, C. A., Dultzin, D., et al., Highly accreting quasars: a tool for cosmology? 2017, in IAU Symposium, Vol. **324**, *IAU Symposium*, 245–246
- Marziani, P. & Sulentic, J. W., Highly accreting quasars: sample definition and possible cosmological implications. 2014, *Mon. Not. R. Astron. Soc.*, **442**, 1211, DOI: 10.1093/mnras/stu951
- Marziani, P., Sulentic, J. W., Dultzin-Hacyan, D., Calvani, M., & Moles, M., Comparative Analysis of the High- and Low-Ionization Lines in the Broad-Line Region of Active Galactic Nuclei. 1996, *ApJS*, **104**, 37, DOI: 10.1086/192291
- Marziani, P., Sulentic, J. W., Plauchu-Frayn, I., & del Olmo, A., Is Mg II 2800 a Reliable Virial Broadening Estimator for Quasars? 2013a, *AAp*, **555**, 89, 16pp
- Marziani, P., Sulentic, J. W., Plauchu-Frayn, I., & del Olmo, A., Low-Ionization Outflows in High Eddington Ratio Quasars. 2013b, *ApJ*, **764** [e-print:[arXiv]1301.0520]
- Mejía-Restrepo, J. E., Lira, P., Netzer, H., Trakhtenbrot, B., & Capellupo, D. M., The effect of nuclear gas distribution on the mass determination of supermassive black holes. 2018, *Nature Astronomy*, **2**, 63, DOI: 10.1038/s41550-017-0305-z
- Mineshige, S., Kawaguchi, T., Takeuchi, M., & Hayashida, K., Slim-Disk Model for Soft X-Ray Excess and Variability of Narrow-Line Seyfert 1 Galaxies. 2000, *Publ. Astron. Soc. Jap.*, **52**, 499, DOI: 10.1093/pasj/52.3.499
- Negrete, A., Dultzin, D., Marziani, P., & Sulentic, J., BLR Physical Conditions in Extreme Population A Quasars: a Method to Estimate Central Black Hole Mass at High Redshift. 2012, *ApJ*, **757**, 62
- Negrete, C. A., Dultzin, D., Marziani, P., et al., Highly accreting quasars: The SDSS low-redshift catalog. 2018, *Astron. Astrophys.*, **620**, A118, DOI: 10.1051/0004-6361/201833285
- Negrete, C. A., Dultzin, D., Marziani, P., & Sulentic, J. W., Reverberation and Photoionization Estimates of the Broad-line Region Radius in Low-z Quasars. 2013, *Astrophys. J.*, **771**, 31, DOI: 10.1088/0004-637X/771/1/31
- Panda, S., Marziani, P., & Czerny, B., The Quasar Main Sequence explained by the combination of Eddington ratio, metallicity and orientation. 2019, *arXiv e-prints*, arXiv:1905.01729
- Peterson, B. M. & Wandel, A., Keplerian Motion of Broad-Line Region Gas as Evidence for Supermassive Black Holes in Active Galactic Nuclei. 1999, *Astrophys. J. Lett.*, **521**, L95, DOI: 10.1086/312190
- Risaliti, G. & Lusso, E., A Hubble Diagram for Quasars. 2015, *Astrophys. J.*, **815**, 33, DOI: 10.1088/0004-637X/815/1/33
- Sadowski, A., Slim accretion disks around black holes, PhD Thesis. 2011, *ArXiv e-prints* [e-print:[arXiv]1108.0396]
- Shen, Y. & Ho, L. C., The diversity of quasars unified by accretion and orientation. 2014, *Nature*, **513**, 210, DOI: 10.1038/nature13712
- Sulentic, J., Marziani, P., & Zamfir, S., The Case for Two Quasar Populations. 2011, *Baltic Astronomy*, **20**, 427

- Sulentic, J. W., Bachev, R., Marziani, P., Negrete, C. A., & Dultzin, D., C IV λ 1549 as an Eigenvector 1 Parameter for Active Galactic Nuclei. 2007, *ApJ*, **666**, 757, DOI: 10.1086/519916
- Sulentic, J. W., del Olmo, A., Marziani, P., et al., What does CIV λ 1549 tell us about the physical driver of the Eigenvector quasar sequence? 2017, *Astron. Astrophys.*, **608**, A122, DOI: 10.1051/0004-6361/201630309
- Sulentic, J. W., Marziani, P., & Calvani, M., An H-R diagram for AGN? 2001, in AIP CP, Vol. **599**, *X-ray Astronomy: Stellar Endpoints, AGN, and the Diffuse X-ray Background*, 963–966
- Sulentic, J. W., Marziani, P., & Dultzin-Hacyan, D., Phenomenology of Broad Emission Lines in Active Galactic Nuclei. 2000, *ARA&A*, **38**, 521, DOI: 10.1146/annurev.astro.38.1.521
- Sulentic, J. W., Zamfir, S., Marziani, P., & Dultzin, D., Our Search for an H-R Diagram of Quasars. 2008, *Revista Mexicana de Astronomia y Astrofisica Conference Series*, **32**, 51
- Tully, R. B. & Fisher, J. R., A new method of determining distances to galaxies. 1977, *Astron. Astrophys.*, **54**, 661
- Vietri, G., The LBT/WISSH quasar survey: revealing powerful winds in the most luminous AGN. 2017, in American Astronomical Society Meeting Abstracts, Vol. **229**, *American Astronomical Society Meeting Abstracts*, 302.06
- Wang, J.-M., Du, P., Valls-Gabaud, D., Hu, C., & Netzer, H., Super-Eddington Accreting Massive Black Holes as Long-Lived Cosmological Standards. 2013, *Physical Review Letters*, **110**, 081301, DOI: 10.1103/PhysRevLett.110.081301